*Wahana Fisika* 10(2) (2025) 90-104

Wahana Fisika

Journal homepage: https://ejournal.upi.edu/index.php/wafi

# Teak Wood (*Tectona grandis*) Sawdust-Derived Activated Carbon: Optimizing Chemical Activation for Physicochemical Properties and Its Potential Relevance to Medical Textile Applications

*Muhamad Taufik Ulhakim[1], Ade Suhara[2], Farah Nadira Noer[1], Bella Kharisma[1], Annissa Novalinda Al-Miraj[1], Rahmad Dian[1], Eki Saputra[1], Rezki Diwanti Suci Lestari[1], Witri Aini Salis[1], Hasna Noer Agus Yayat[1]*

[1]Politeknik STTT Bandung, Jl. Jakarta No. 31, Bandung, West Java

[2]Department of Industrial Engineering, Faculty of Engineering, Universitas Buana Perjuangan Karawang, Jl. HS Ronggowaluyo, Karawang, West Java

* Corresponding author. E-mail: *taufik-ulhakim@kemenperin.go.id*

## ABSTRACT

This study investigated the synthesis of activated carbon (AC) from teak wood (Tectona grandis) sawdust using three chemical activating agents: phosphoric acid ($H_3PO_4$), hydrochloric acid (HCl), and sodium hydroxide (NaOH). The effects of these agents on the physicochemical properties and adsorption performance of the resulting AC were systematically evaluated. $H_3PO_4$ produced AC with the most favorable characteristics, exhibiting a high adsorption capacity, as indicated by an iodine number of approximately 943 mg/g. This reflects a well-developed microporous structure with high surface area, suitable for adsorbing small molecules, such as malodorous compounds in wound exudates. The results highlight the potential of $H_3PO_4$-activated AC for medical textile applications. Further in situ studies are recommended to validate its performance in real wound environments.

## ARTICLE INFO

***Article History:***

*Submitted November 2025*
*Accepted December 2025*
*Available online December 2025*
*Publication Date Dec 8, 2025*

***Keyword:***

*Teak wood sawdust (TWS); activated carbon (AC); chemical activation; iodine number; medical textile applications*

## 1. Introduction

The pressing global issues of sustainability demand innovations in environmentally friendly materials, not only for general industries but also for the healthcare industry. This encompasses the non-implant medical textile sector, including compression garments for burn therapy [1], wound dressings [2], textile-based plasters [3], and sterile gauze [4]. At present, the healthcare industry has a tendency to utilise fossil-based synthetic materials. It is widely accepted that, in the long term, these materials may lead to a range of environmental and health problems. Therefore, it is imperative that they be replaced with alternatives that are renewable, environmentally friendly, and safe. One promising material for such applications is activated carbon (AC).

AC has been shown to function effectively as an absorber of odours, smoke, and chemical gases, thereby enhancing wearer comfort [5]. In practice, the utilisation of AC for non-implant medical textile applications can be achieved through several approaches, including coating the fabric surface, impregnating it into textile fibres, or inserting it as a middle layer in a sandwich structure [6]. The use of AC is underpinned by its numerous advantages, such as a high surface area, substantial adsorption capacity, and the possibility of being produced from local natural resources or biomass [7].

One abundant biomass with great potential to be utilised as a source of AC is agricultural waste. This aligns with Indonesia's position as an agrarian country that generates large quantities of agricultural residues every year [8]. Among these, teak wood sawdust (TWS) is one of the most abundant by-products, generated in significant volumes from the wood processing and furniture industries [9]. The accumulation of this waste poses environmental challenges, including disposal problems and the risk of air and soil pollution, which highlights the urgency of proper management and valorisation [10]. With its high lignocellulosic content and favourable physicochemical properties, TWS represents a promising precursor for AC production.

Several studies have reported the synthesis of AC from TWS using different chemical activating agents. Mekibes *et al.* (2024) demonstrated that activation with $H_3PO_4$ effectively developed a porous network, resulting in a high surface area and enhanced adsorption capacity, particularly for organic pollutants decontamination [11]. Alam *et al.* (2020) showed that activation with HCl improved the removal of inorganic impurities and facilitated the formation of mesopores, thereby improving performance in various applications [12]. Meanwhile, Arman *et al.* (2024) highlighted that

activation with NaOH increased carbon yield and created well-developed micropores, which enhanced its suitability for pyrolysis [13].

These findings consistently suggest that the choice of chemical activating agent between $H_3PO_4$, HCl, or NaOH plays a crucial role in determining the physicochemical properties of TWS-derived AC, particularly with respect to pore development, surface chemistry, and adsorption performance. However, to date, no comprehensive study has directly compared these three chemical agents under identical synthesis conditions to systematically evaluate their effects on AC based TWS production. This represents a critical gap in the literature that must be addressed in order to identify the optimal activation pathway for high-performance AC production.

Therefore, the present study aims to compare the performance of TWS-derived AC synthesized using $H_3PO_4$, HCl, and NaOH under the same conditions, with the objective of identifying the most effective activating agent and synthesis parameters. The expected outcome of this research is to establish an efficient and sustainable route for producing high-quality AC. In the future, such AC materials could be further developed for advanced applications in the healthcare sector, particularly in non-implant medical textiles such as wound dressings with odour-adsorbing functionality. This innovation is anticipated to improve patient comfort, reduce wound-related complications, and contribute to the development of eco-friendly medical products.

## 2. Materials and Methods

### 2.1. Preparation of TWS-AC

TWS were employed as natural resources for the synthesis of AC due to its abundance of carbon elements, as reported by Cansado *et al*. in 2022 [14], Negara *et al*. in 2023 [15], and Sutapa *et al*. in 2024 [16]. The percentage of carbon and other elements in the TWS is shown in Table 1. The TWS was collected from local furniture industry around Karawang, Indonesia.

Table 1. Elements contained in the TWS [17].

| Elements | Percentage (%) |
|---|---|
| Carbon (C) | 57.0 |
| Oxygen (O) | 10.5 |
| Manganese (Mn) | 6.0 |
| Calcium (Ca) | 3.0 |
| Iron (Fe) | 3.0 |
| Potassium (K) | 6.0 |
| Silica (Si) | 14.5 |

TWS was then subjected to a synthesis process to produced AC through chemical activation. The chemical activation of carbonaceous materials was carried out using phosphoric acid ($H_3PO_4$) (AC-1), hydrochloric acid (HCl) (AC-2), and sodium

DOI: https://doi.org/10.17509/wafi.v10i2.91992
e- ISSN 2549-1989

hydroxide (NaOH) (AC-3). The expected outcome of this process was the formation of AC with favorable properties suitable for medical textile applications, one of which is its ability to absorb wound exudate, thereby accelerating the reduction of wound area [18].

The synthesis process is illustrated in Figure 1, which was adapted from Lobato-Peralta's work published in 2025 [19]. Firstly, TWS was washed and sun-dried for approximately 3 days to reduced its water content. This was followed by a pre-carbonization process at 400 °C for 2 hours. The sample produce was subjected to a crushing and sieving process using a 200-sieve, with the objective of obtaining a uniform particle size. Subsequently, the sample was chemically activated using the three different activating agents under identical conditions to yield AC with optimal properties for medical textile application. Each sample was mixed with the activating agent at a 1:2 ratio. It is then stirred with a magnetic stirrer at 600 rpm for 2 hours and then left to stand for 36 hours to obtain the residue. The residue was washed with demineralized water until the pH reached 7. The samples were then dried at 100 °C for 5 hours in a muffle furnace to remove residual moisture. Finally, the dried samples were subjected to activation at 650 °C for 1 hour, followed by crushing and sieving to obtain AC with a uniform particle size.

## 2.2. Characterization of TWS-AC

The AC was then characterized to ascertain its suitability as a wound exudate-absorbing material or as a supporting material in medical textiles. To evaluated the AC properties, X-ray diffraction (XRD) and Scanning electron microscopy coupled with energy dispersive x-ray (SEM-EDX) were employed to identify specific characteristics, including crystallinity or amorphicity [20], as well as the elemental composition of AC [21]. Then, as reported by Forss *et al*. (2022), the AC used for wound exudate odour control must possess a high absorption capacity to effectively reduce odour release from the wound [22]. In addition, the physical properties of AC are fundamental indicators for evaluating its quality, including of carbon yield, bulk density, ash content, moisture content, volatile matter, and FCC. Also, the absorption capacity of AC is evaluated through the iodine number determination. This analysis was conducted simultaneously to determine the optimal chemical activation for producing AC with superior properties, particularly for wound exudate odour absorption.

### 2.2.1. Carbon Yield and Bulk Density

The quantification of carbon yield is achieved through the application of Equation

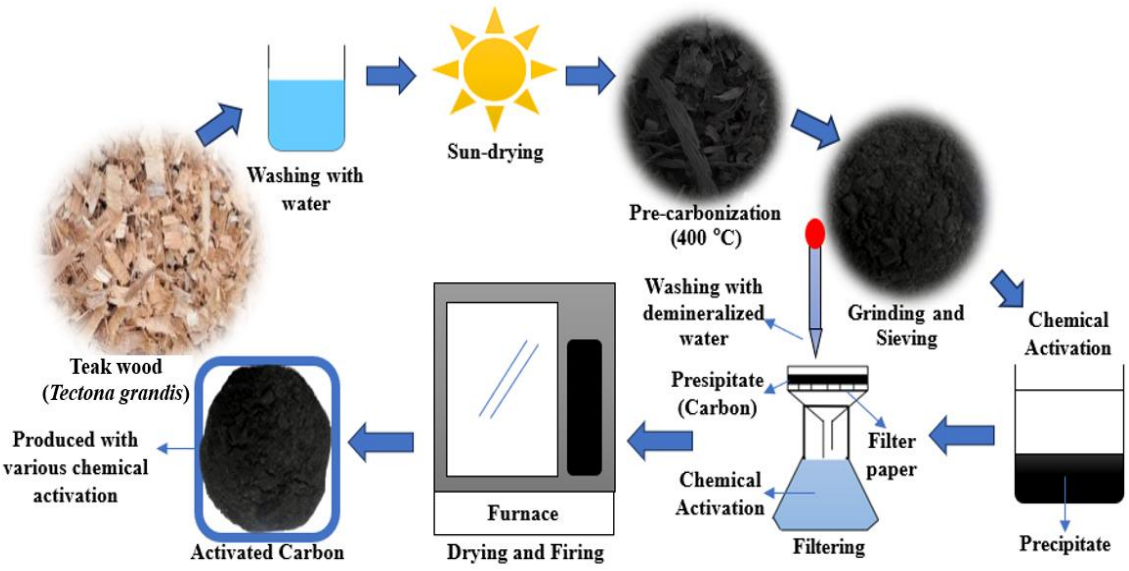


Figure 1. Illustration of activated carbon synthesis.

(1). The carbon yield is defined as the ratio of the weight of AC to the weight of raw material [23]. The weighing is conducted prior to the raw material undergoing pre-carbonization and subsequent to the production of AC. This process are conducted using electronic analytical balances.

$$\text{Carbon yield (\%)} = \frac{W_{AC}}{W_{RM}} \text{ x } 100\% \qquad (1)$$

where $W_{AC}$ is the mass of AC recorded at the end of the process (g) and $W_{RM}$ is the mass of raw material (g), the raw material used in this work is TWS.

Then, the bulk density of AC is identified through the Equation (2) [23]. The process is conducted following the standart of ASTM D2854 [24] with slight modification. This measurement was performed with the AC added to the tube with the volume and mass as previously known.

$$\text{Bulk density} = \frac{\text{weight of AC (g)}}{\text{volume of AC (ml)}} \qquad (2)$$

### 2.2.2. Ash Content

The ash content of AC is evaluated according to the standart ASTM method, which is ASTM D2866 [25]. It was then determined using Equation (3) [26]. The procedure was started by weighing the crucible with the lid. Then, 1.0 g of AC is weighed into a crucible and subjected to heating using a furnace at 650 °C for 1 hour. The crucible is then cooled to room temperatur and reweighed.

$$\text{Ash Content (\%)} = \frac{m_{final}}{m_{initial}} \text{ x } 100\% \qquad (3)$$

where $m_{initial}$ and $m_{final}$ are respectively initial and final mass that recorded in this characterization process.

DOI: https://doi.org/10.17509/wafi.v10i2.91992
e- ISSN 2549-1989

### 2.2.3. Moisture Content

The moisture content is determined according to the Equation (4). 1.0 g of AC is placed in the crucible and dried at 150 °C for 3 hours. This process is following the standard of ASTM series number D2867 [27]. The sample is then weighed after the whole process [28].

$$\text{Moisture content (\%)} = \frac{W_1 - W_2}{W_1} \text{ x } 100\% \quad (4)$$

where $W_1$ is the mass of AC before drying (g) and $W_2$ is the mass of AC after drying (g).

### 2.2.4. Volatile Matter

Volatile matter is determined by ASTM standard D5832 according to the procedure performed by Ngernyen in 2020 [29]. 1.0 g of AC is heated at 950 °C for 30 minutes. It was then cooled to room temperature. The weight loss in before and after heating treatment is volatile matter. The volatile matter was then calculated using Equation (5) below [30]:

$$\text{Volatile matter (\%)} = \frac{[100(B-F)-M(B-G)]}{(B-G)(100-M) \text{ x } 100} \quad (5)$$

Where B is the mass of the crucible with AC before heating (g), F is the mass of the crucible with AC after heating (g), G is the mass of the crucible (g), and M is the moisture content of the AC.

### 2.2.5. Fixed Carbon Content

The FCC of AC derived from TWS that has been done in this work was calculated using Equation (6) as follows [31]:

$$\text{FCC} = 100\% - (\%M + \%A + \%VM) \quad (6)$$

Where %M is the moisture content of the AC, %A is the ash content of the AC, and %VM is the volatile matter of the AC.

### 2.2.6. Iodine Number

The iodine number test is a significant parameter in AC, as it is utilised to evaluate its capacity to absorb small molecules [32]. It has been demonstrated that the iodine number value is directly proportional to the AC's capacity for the absorption of small compounds. In the domain of medical textiles, its application in wound dressings is advantageous due to its capacity to absorb malodorous volatile organic compounds emanating from wounds. Consequently, an elevated iodine number is indicative of the remarkable capacity of AC to mitigate odours in wounds.

Then, the iodine number test was conducted with reference to ASTM D4607-94 [33]. 1.0 g of AC was meticulously prepared and subsequently introduced into an Erlenmeyer flask containing 10 ml of 5% HCl. The contents of the flask were then boiled for 30 sec and cooled to room temperature. Then, 100 ml of iodine solution with a concentration of 0.1 M was introduced and agitated for a period of approximately 30 min before being filtered. In the next step, 25 ml of the filtrate was taken and titrated with sodium thiosulfate ($Na_2S_2O_3$) at a

concentration of 0.1 M and using starch as an indicator.

## 3. Results and Discussions

The XRD pattern represents AC derived from TWS that was chemically activated using different agents: $H_3PO_4$ (black), HCl (red), and NaOH (blue), as shown in Figure 2. The broad peaks observed in the range of $2\theta = 20°–30°$ correspond to the characteristic region of amorphous carbon. The lack of sharp diffraction peaks indicates that the TWS-derived activated carbon possesses predominantly amorphous structures rather than crystalline phases [34].

The peak positions slightly vary depending on the activating agent: $H_3PO_4$ at around 23.0°, HCl at approximately 23.5°, and NaOH at about 24.0°. These small shifts suggest differences in the structural arrangement of carbon layers, where NaOH activation tends to produce a slightly more compact arrangement compared to HCl and $H_3PO_4$.

Overall, the results confirm that TWS-derived AC exhibits amorphous characteristics, which are advantageous for adsorption processes. The disordered carbon structure enhances porosity and surface area, making the material highly suitable for applications such as medical textiles, where efficient absorption of wound exudates and toxic compounds is required [35].

The SEM micrographs of TWS-derived AC in Figure 3(a), 3(b), and 3(c) show irregular and porous morphologies characterized by fractured surfaces, rough textures, and scattered voids. These structural features are consistent with the amorphous nature confirmed by the XRD results. When compared to the reference micrograph in Figure 3(d), notable similarities and differences can be observed. Both sets of images display irregular particle shapes and the absence of long-range order, confirming the amorphous character of the carbon materials. However, Figure 3(a)-(c) exhibit more pronounced pore openings and fragmented structures, suggesting the development of higher surface irregularities and potentially greater surface area compared to the reference. In contrast, the reference sample in Figure 3(d) shows relatively larger, compact, and aggregated particles, with less visible porosity at the same scale. This comparison highlights that TWS-derived AC develops a porous morphology comparable to the general characteristics of amorphous carbons but with more fragmented and irregular features, which may provide

DOI: https://doi.org/10.17509/wafi.v10i2.91992
e- ISSN 2549-1989

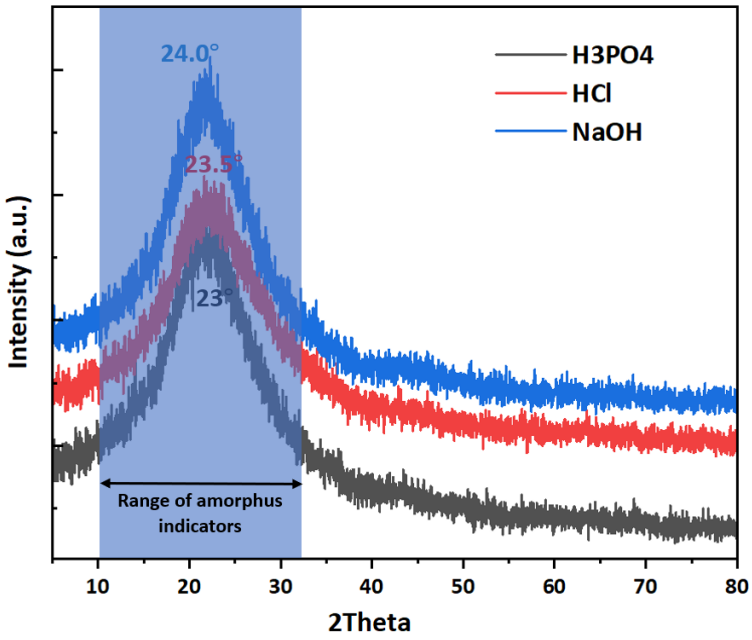


Figure 2. XRD pattern of TWS-derived AC with different chemical activation: (a) $H_3PO_4$, (b) HCl, (c) NaOH.

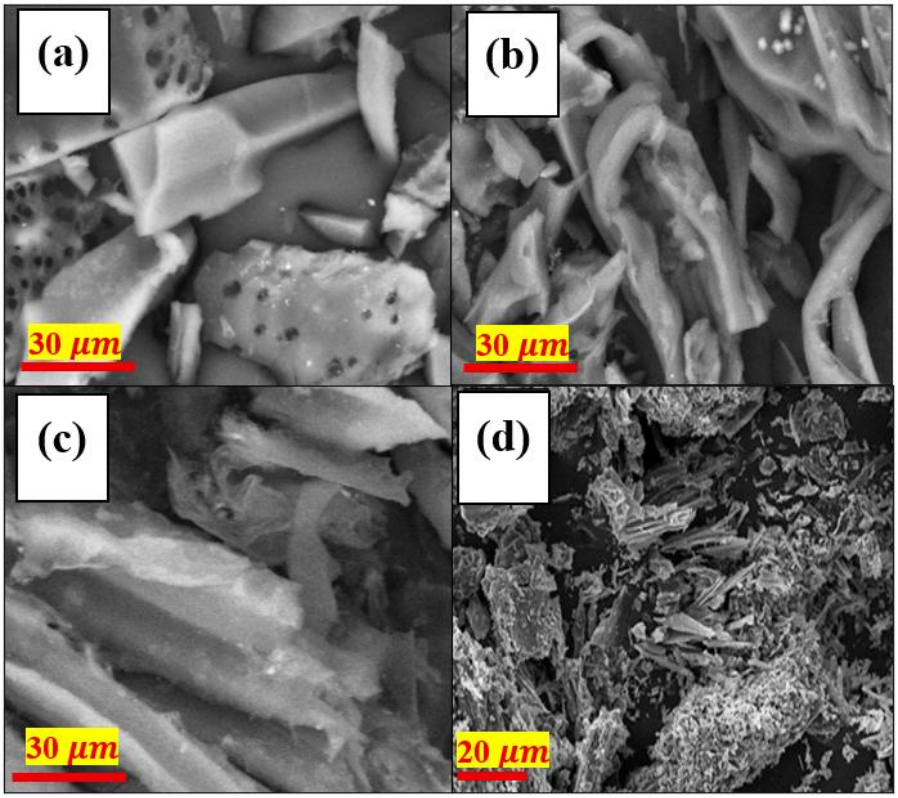


Figure 3. SEM image of TWS-derived AC with different chemical activation: (a) $H_3PO_4$, (b) HCl, (c) NaOH, and (d) reference [36].

superior adsorption potential for applications such as medical textiles requiring efficient fluid absorption and retention.

Then, the EDX evaluation shown that $H_3PO_4$ (AC-1), HCl (AC-2), and NaOH (AC-3) have a percentage of carbon element more than 60% as shown in Table 2, it indicates the successful of synthesis process. Carbon and oxygen dominate all samples, confirming the typical composition of AC.

Table 2. Element contain in AC derived from TWS (this work)

| **Elements** | **Percentage (%)** | | |
|---|---|---|---|
| | **AC-1** | **AC-2** | **AC-3** |
| Carbon (C) | 75.8 | 74.2 | 72.4 |
| Oxygen (O) | 20.2 | 21.5 | 23.1 |
| Manganese (Mn) | 0.3 | 0.2 | 0.4 |
| Calcium (Ca) | 0.8 | 0.9 | 0.6 |
| Iron (Fe) | 0.6 | 0.5 | 0.5 |
| Potassium (K) | 1.5 | 2.2 | 1.8 |
| Silica (Si) | 0.8 | 0.5 | 1.2 |

AC-1 ($H_3PO_4$ activation) shows the highest carbon content (75.8%), indicating good carbon retention after activation, while its oxygen content (20.2%) suggests the presence of oxygenated functional groups that can enhance adsorption properties. AC-2 (HCl activation) has slightly lower carbon (74.2%) but a marginally higher oxygen content (21.5%) compared to AC-1, with the highest potassium content (2.2%), likely originating from residual inorganic minerals. AC-3 (NaOH activation) exhibits the lowest carbon content (72.4%) but the highest oxygen percentage (23.1%), indicating more surface functionalization that may contribute to increased hydrophilicity, although excessive oxygen groups may also reduce structural stability [37].

Minor elements such as Mn, Ca, Fe, K, and Si are present in small amounts, reflecting the natural inorganic composition of TWS and the influence of activating agents. These mineral traces may also contribute to surface heterogeneity and adsorption activity. Among the samples, AC-1 demonstrates a balanced composition with high carbon content and sufficient oxygen, making it the most favorable for adsorption applications. The combined presence of carbon stability and functional groups enhances its potential use in medical textiles, where both porosity and hydrophilicity are crucial for wound exudate absorption and antibacterial performance.

To validating this performance of AC, the several physicochemical properties test are conducted. The physicochemical properties of the AC synthesized using different chemical activating agents are summarized in Table 3. The yield values ranged from 28.7% to 35.2%, with AC-3 (NaOH) exhibiting the highest yield, followed by AC-1 ($H_3PO_4$) and AC-2 (HCl). A higher yield is favourable for large-scale production as it ensures greater material

DOI: https://doi.org/10.17509/wafi.v10i2.91992
e- ISSN 2549-1989

efficiency, which is highly beneficial for sustainable applications in medical textiles [38]. The bulk density of the samples varied between 0.47 and 0.52 g/ml, indicating a moderate density suitable for integration into textile substrates without causing excessive weight or compromising wearer comfort. Ash content was lowest in AC-2 (4.2%), implying fewer inorganic residues and more effective adsorption performance, which is crucial for the removal of odor-causing compounds in wound dressings [39]. Moisture content for all ACs was relatively low (5.9–6.8%), remaining below the recommended 10% threshold, thereby ensuring material stability and minimizing microbial growth when applied in moist wound environments. The volatile matter content showed a noticeable difference, with AC-1 having the lowest value (17.6%), suggesting a greater development of porosity and stability compared to AC-2 (20.1%). Finally, the fixed carbon content (FCC) of all samples was consistently high, ranging from 69.5% to 69.8%, reflecting a stable carbon framework capable of supporting high adsorption capacity.

These results highlight that AC-1 ($H_3PO_4$) demonstrates the most balanced properties, with high yield, moderate bulk density, low volatile matter, and high fixed carbon content, making it a strong candidate for medical textile applications such as odor-adsorbing wound dressings. Meanwhile, AC-2 (HCl), with its low ash content, also presents significant potential for maximizing adsorption performance. Overall, the findings indicate that TWS-derived AC possess suitable physicochemical characteristics for non-implant medical textile applications, particularly in enhancing patient comfort and accelerating the wound-healing process through effective odor and moisture management.

Table 3. Physicochemical properties of AC

| **Indicators** | **AC-1** | **AC-2** | **AC-3** |
|---|---|---|---|
| Yield (%) | 35.2 | 28.7 | 32.5 |
| Bulk density (g/ml) | 0.50 | 0.47 | 0.52 |
| Ash Content (%) | 6.1 | 4.2 | 5.8 |
| Moisture Content (%) | 6.8 | 5.9 | 6.3 |
| Volatile Matter (%) | 17.6 | 20.1 | 18.4 |
| FCC (%) | 69.5 | 69.8 | 69.5 |

The iodine number analysis, as presented in Figure 4, reveals significant differences in the adsorption capacity of the three types of activated carbon (AC). AC-1, synthesized using $H_3PO_4$, exhibited the highest iodine number of 943 mg/g, indicating a highly developed porous structure and large surface area, which directly enhances its ability to adsorb small molecules. AC-2, prepared with HCl, showed a moderate iodine number of 782 mg/g, suggesting an intermediate level of porosity and adsorption capability. Meanwhile, AC-3, derived using NaOH, had the lowest iodine

number of 661 mg/g, reflecting a less developed porous network compared to the other two samples. These results confirm that the choice of activating agent plays a crucial role in determining the surface chemistry and porosity of AC. The superior performance of AC-1 suggests that $H_3PO_4$ activation is more effective in producing microporous structures suitable for adsorption of low-molecular-weight compounds [40]. In the context of medical textile applications, particularly for odor-absorbing wound dressings, a higher iodine number is advantageous as it ensures more effective adsorption of volatile compounds and exudates, thereby improving patient comfort and potentially accelerating the healing process.

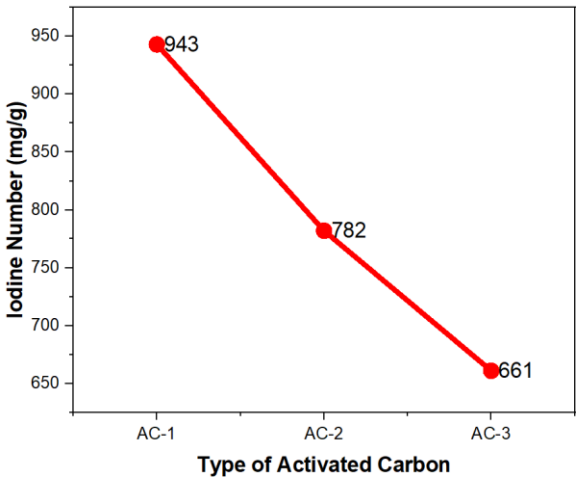


Figure 4. Iodine number of each AC samples.

## 4. Conclusions

This work investigated the preparation of AC using three different chemical activating agents: $H_3PO_4$, HCl, and NaOH. The effects of these agents on the physicochemical properties of the resulting AC were systematically evaluated. The results indicate that $H_3PO_4$ produced the most superior AC, particularly in terms of adsorption capacity, as evidenced by an iodine number of approximately 943 mg/g. A high iodine number reflects excellent micropore development and adsorption potential, suggesting that this AC is highly suitable for applications requiring the removal of small molecules, such as the adsorption of malodorous compounds in wound exudates. Further studies are recommended to directly assess the performance of this AC in real wound environments, which would provide more robust validation of its effectiveness for medical textile applications.

## 5. Acknowledgement

The authors gratefully acknowledge the support and facilitation provided by Politeknik STTT Bandung, under the Ministry of Industry of the Republic of Indonesia.

## 6. References

[1] DeBruler, D. M, dkk. (2020). Improved Scar Outcomes with Increased Daily Durationof Pressure Garment Therapy. *Advances in Wound Care Vol. 9, No. 8,* 453-461.

DOI: https://doi.org/10.17509/wafi.v10i2.91992
e- ISSN 2549-1989

[2] Su, L, dkk. (2023). The Emerging Progress on Wound Dressings and Their Application in Clinic Wound Management. *Heliyon Vol. 9, e22520,* 1-13.

[3] Li, Y, dkk. (2024). Bioactive Electrospun Nanoyarn-constructed Textile Dressing Patches Delivering Chinese Herbal Compound for Accelerated Diabetic Wound Healing. *Materials & Design Vol. 237, 112623,* 1-15.

[4] Sheng, K, dkk. (2025). Cotton Gauze Fabricated with Hydro-stable Zn-MOF Enables Hemostatis Acceleration, Antibacterial Activity, and Wound Regeneration. *International Journal of Biological Macromolecules Vol. 316, 144654,* 1-13.

[5] Ramadhani, L. F, dkk. (2020). Review: Teknologi Aktivasi Fisika pada Pembuatan Karbon Aktif dari Limbah Tempurung Kelapa. *Jurnal Teknik Kimia Vol. 26, No. 2,* 42-53.

[6] Sing, K, dkk. (2024). A Comprehensive Review on Activated Carbon Fabrics: Preparation, Characterization, and Applications in Electromagnetic Interference Shielding and Joule Heating. *Journal of Analytical and Applied Pyrolysis Vol. 182, 106689,* 1-22.

[7] Manurung, M, dkk. (2025). Karbon Aktif dari Bahan Alam sebagai Adsorben Ramah Lingkungan: Potensi, Tantangan, dan Aplikasinya. *Journal of Environmental Engineering Inovation Vol. 2, No. 1,* 38-48.

[8] Budiarto, A, dkk. (2023). Pengolahan Limbah Pertanian sebagai Pakan Ternak di Kawasan Transmigrasi Uluklubuk Kabupaten Malaka. *ABDI UNISAP: Jurnal Pengabdian Kepada Masyarakat Vol. 1, No. 2,* 123-130.

[9] Indrawan, D. A, dkk. (2024). Assessing the Potential Utilization of Super Teak for Furniture, Flooring, Veneer, Pulp Paper and Wood Pellets. *AIP Conference Proceedings Vol. 2973, No. 1*, March 2024.

[10] Tawo, O. E, dkk. (2025). Advancing Waste Valorization Techniques for Sustainable Industrial Operations and Improved Environmental Safety. *International Journal of Science and Research Archive Vol. 14, No. 2,* 127-149.

[11] Mekibes, Z, dkk. (2024). Activator Effect on Sawdust-based Adsorbent Efficiency: Application to Organic Pollutants Decontamination. *Studies in Engineering and Exact Sciences, Curitiba Vol. 5, No. 1,* 847-875.

[12] Alam, M. M, dkk. (2020). The Potentiality of Rice Husk-Derived Activated Carbon: From Synthesis to Application. *Processes Vol. 8, No. 2,* 203.

[13] Arman, M, dkk. (2024). The Effect of Pyrolisis Temperature on Sawdust-Biomass Activated Carbon Using NaOH and NaCl Activators. *Environment, Energy and Natural Resources Vol. 28, No. 8,* 1-11.

[14] Cansado, I. P, dkk. (2022). Using Tectona Grandis Biomass to Produce Valuable Adsorbents for Pesticide Removal from Liquid Effluent. *Materials Vol. 15, No. 5842,* 1-15.

[15] Negara, D. N. K. P, dkk. (2023). The Effect of Carbonisation Heating Rates on the Properties of N-Doped Teak Sawdust Waste Activated Carbon. *Journal of Physical Science Vol. 34, No. 3,* 1-20.

[16] Sutapa, J. P. G, dkk. (2024). Conversion of Shoot Waste of Fast-Growing Teak into Activated Carbon and Its Adsorption Properties. *Journal of the Korean Wood Science and Technology Vol. 52, No. 5,* 488-503.

[17] Okon-akan, O, dkk. (2022). Characterization of Activated Carbon Produced from Teak (*Tectona grandis*) Sawdust. *PRO LIGNO Vol. 18, No. 3,* 21-25.

[18] Probst, S, dkk. (2022). Superabsorbent Charcoal Dressing versus Silver Foam Dressing in Wound Area Reduction: A Randomised Controlled Trial. *Journal of Wound Care Vol. 31, No. 2,* 140-146.

[19] Lobato-Peralta, D. R, dkk. (2025). Evaluating the Impact of Pre-carbonization on Activated Carbon Production from Animal-origin Precursors for Supercapasitor Electrode Applications. *Biomass and Bioenergy Vol. 193, 107574,* 1-10.

[20] Iwanow, M, dkk. (2020). Activated Carbon as Catalyst Support: Precursores, Preparation, Modification and Characterization. *Beilstein Journal of Organic Chemistry Vol. 16,* 1188-1202.

[21] Sujiono, E. H, dkk. (2022). Fabrication and Characterization

DOI: https://doi.org/10.17509/wafi.v10i2.91992
e- ISSN 2549-1989

of Coconut Shell Activated Carbon using Variation Chemical Activation for Wastewater Treatment Application. *Results in Chemistry Vol. 4, 200291,* 1-10.

[22] Forss, J. R, dkk. (2022). The Properties of an Activated Carbon-containing Agarose Film for the Amelioration of 2-amino Acetophenone Malodour as Produced in Chronic Wounds Infected with Pseudomonas aeruginosa. *Journal of Materials Science Vol. 57,* 16460-16470.

[23] Mkungunugwa, T, dkk. (2021). Synthesis and Characterisation of Activated Carbon Obtained from Marula (Sclerocarya birrea) Nutshell. *Journal of Chemistry Vol. 2021, ID 55552224,* 1-9.

[24] Gomma, M, B. (2022). Possibility of using Olive-seeds Residues as a Source of Activated Carbon. *Al-Azhar Journal of Agricultural Engineering Vol. 2,* 10-16.

[25] Serafin, J, dkk. (2023). Biomass Waste Fern Leaves as a Material for a Sustainable Method of Activated Carbon Production for $CO_2$ capture. *Biomass and Bioenergy Vol. 175, 106880,* 1-10.

[26] Harlette, P. Z, dkk. (2023). Enhanced Adsorption of Toluene using Nano Silver-Modified Activated Carbon Derived from *Ricinodendron heudolitii* Shells: A Comparative Study. *Hybrid Advanced Vol. 4, 100098,* 1-13.

[27] Koochaki, C. B, dkk. (2020). The Effect of Pre-swelling on the Characteristics of Obtained Activated Carbon from Cigarette Butts Fibers. *Biomass Conversion and Biorefinery Vol. 10,* 227-236.

[28] Jawad, A. H, dkk. (2020). Insight Into the Modeling, Characterization and Adsorption Performance of Mesoporous Activated Carbon from Corn Cob Residue *via* Microwave-Assisted $H_3PO_4$ Activation. *Surface and Interfaces Vol. 21, 100688,* 1-11.

[29] Ngernyen, Y, dkk. (2020). Low Cost Activated Carbon Prepared from *Dipterocarpus alatus* Fruit. *Science & Technology Development Journal – Engineering and Technology Vol. 13, No. S13,* S175-S180.

[30] Njewa, J. B, dkk. (2022). Synthesis and Characterization of Activated Carbons Prepared from Agro-wastes by Chemical Activation. *Journal of Chemistry Vol. 2022, ID 9975444*, 1-13.

[31] Ashtaputrey, P. D, dkk. (2020). Preparation and Characterization of Activated Charcoal Derived

from Wood Apple Fruit Shell. *Journal of Scientific Research Vol. 64, No. 1,* 336-340.

[32] Paulino, R, dkk. (2023). Critical Review of Adsorption and Biodegradation Mechanisms for Removal of Biogenic Taste and Odour Compounds in Granular and Biological Activated Carbon Contactors. *Journal of Water Process Engineering Vol. 52, 103518,* 1-15.

[33] Zurizam, N. A. F, dkk. (2025). Performance of Activated Carbon from Cassava Peel for the Removal of Pb(II) in Pb Solution. *Journal of Academia Vol. 13, No. 1,* 34-42.

[34] Moseenkov, S. I, dkk. (2023). Investigation of Amorphous Carbon in Nanostructured Carbon Materials (A Comparative Study by TEM, XPS, Raman Spectroscopy and XRD). *Materials Vol. 16, No. 3,* 1112.

[35] Antunes, J, dkk. (2021). Carbon-Based Coatings in Medical Textiles Surface Functionalisation: An Overview. *Processses Vol. 9, No. 11,* 1997.

[36] Singh, J, dkk. (2020). Synthesis and Characterization od Activated Carbon Derived from Tectona Grandis Sawdust via Green Route. *Environmental Progress & Sustainable Energy Vol. 40, No. 2,* e13525.

[37] Jha, M. K, dkk. (2021). Surface Modified Activated Carbons: Sustainable Bio-Based Materials for Environmental Remediation. *Nanomaterials Vol. 11, No. 11,* 3140.

[38] Patti, A, dkk. (2022). Towars the Sustainability of the Plastic Industry through Biopolymers: Properties and Potential Applications to the Textile World. *Polymers Vol. 14, No. 4,* 692.

[39] Hossains, M. T, dkk. (2025). Progress and Prospects of Chemical Functionalization Textiles via Nanotechnology. *ACS Applied Engineering Materials Vol. 3, No. 1,* 1-20.

[40] Elamraoui, S, dkk. (2025). Comparative Study of Raw Pinus Sylvestris Sawdust and Its Activated Carbon for Chemical Oxygen Demand and Polyphenols Removal from Olive Mill Wastwater. *Biomass Conversion and Biorefinery,* Publish in March 2025.

DOI: https://doi.org/10.17509/wafi.v10i2.91992
e- ISSN 2549-1989